Resonant transfer and excitation in collisions of C^{5+} with H_2 and He targets

R. Parameswaran, C. P. Bhalla, B. P. Walch, and B. D. DePaola
J. R. Macdonald Laboratory, Kansas State University, Manhattan, Kansas 66506-2604
(Received 22 January 1991)

Auger electrons emitted from doubly excited states of $C^{4+}(2l2l',2l3l',2l4l',2l5l')$ formed by transfer excitation in collisions of C^{5+}(4–10 MeV) with H_2 and He were studied using high-resolution zero-degree Auger electron spectroscopy. The *KLL*, *KLM*, *KLN*, and *KLO* resonant-transfer excitation (RTE) cross sections were measured. The impulse approximation theory with alignment and interference effects taken into consideration was found to be in reasonable agreement with the experimental data. The theory was normalized by a typical factor of 0.65 to obtain the best fits to the data. The RTEA resonance strengths were evaluated to investigate the n dependence ($n=2,3,4,5$) of RTEA, which is RTE followed by Auger electron emission.

I. INTRODUCTION

Resonant-transfer-excitation (RTE) is a two-electron process in energetic ion-atom collisions, where a projectile ion captures a target electron and simultaneously one electron in the projectile gets excited resulting in doubly excited intermediate states $2lnl'$. This process has been studied for a number of different collision systems.[1–4] When the projectile ion decays through Auger emission, the process is termed RTEA.

Previous RTEA experiments[1,3,4] using state-selective high-resolution Auger electron spectroscopy have looked only at the *KLL* Auger electrons for O^{5+}, F^{6+}, F^{8+} on He and H_2 and have reported results generally in good agreement with the angular-dependent impulse approximation theory.[5] Schulz *et al.*[6] studied the *KLL*, *KLM*, *KLN*, and *KLO* RTEA cross section for $F^{8+}+H_2$, but without quantitative comparisons with theory. In this paper we report on an extensive study of the RTEA process in collisions of C^{5+} in the energy range of 4–10 MeV with H_2 and He targets. We present comparison between theory and experiment for the *KLL*, *KLM*, *KLN*, and *KLO* differential RTEA cross sections at zero-degree observation angle. The corresponding atomic parameters for the doubly excited C^{4+} were calculated using the Hartree-Fock atomic model. The comparison is made by determining the RTEA resonance strengths, which is the RTEA cross section integrated over the range of projectile energy, for the different *KLn* cross sections.

In Sec. II the experiment and data analysis scheme are given. The theory is presented in Sec. III. The experimental results are discussed in Sec. IV and the summary is presented in Sec. V.

II. EXPERIMENT

The experimental setup has been described previously.[7] Briefly, it consists of a gas target cell followed by a zero-degree, tandem, parallel-plate electron spectrometer and channeltron electron multiplier. Hydrogenlike carbon projectiles were produced using the 7-MV EN tandem Van de Graaff accelerator at the J. R. Macdonald Laboratory at Kansas State University. Auger electrons emitted along the projectile axis, subsequent to collision with the target, were energy analyzed using the electron spectrometer.

Typical electron spectra at a projectile energy of 7.5 MeV are shown in Fig. 1. In Figs. 1(a) and 1(d), sitting on top of the smoothly varying binary-encounter electron background are the *KLL*, *KLM*, and *KLN*, and higher-order Auger electron contributions up to the $2lnl'$ series limit. The spectra have been normalized using the measured ion current and charge state, the spectrometer solid angle and efficiency, and spectrometer dispersion. In a recent publication,[3] it was shown that the binary-encounter electrons afford a convenient method for absolute efficiency determination of a tandem zero-degree electron spectrometer and were used in this experiment for absolute normalization at each projectile energy. The laboratory-frame spectra in Figs. 1(a) and 1(d) after being transformed to the projectile frame are shown in Figs. 1(b) and 1(e). The binary-encounter electron backgrounds are subtracted from Figs. 1(b) and 1(e) after first being fitted to smooth curves. The normalized, transformed and background subtracted spectra are shown in Figs. 1(c) and 1(f). An analysis scheme similar to that outlined above was adopted at each projectile energy and representative electron spectra are shown in Fig. 2 for 6-, 7-, 8-, and 9-MeV projectile energies.

The spectrometer resolution was sufficient to resolve the individual *KLL*, *KLM*, *KLN*, and *KLO* contributions but not the detailed structure within each manifold. However, TE is the only possible mechanism for Auger electron production for the hydrogenlike C^{5+} projectiles and according to theory $2p^2\,{}^1D$ should be the dominant line in the *KLL* manifold. This was experimentally verified for the *KLL* manifold for the F^{8+} and H_2 collision system.[4] The contributions of $2pnp\,{}^1D$ and $2snd\,{}^1D$ are expected to be dominant for other *KLn* manifolds. Double capture is negligible at the projectile energies studied, for these collision systems.

III. THEORY

The RTEA process in ion-atom collision is a process involving the transfer of a target electron to the projectile with the simultaneous excitation of the projectile electron thus forming the doubly excited autoionizing states that deexcite by Auger electron emission. This phenomenon is analogous to the electron-ion collision wherein autoionizing states appear as resonances in elastic scattering. The connection between the two processes is made through the use of the impulse approximation, when the projectile velocity is much larger than the typical velocity of the target atom, as originally proposed by Brandt.[8] Using the recently developed formalism by Bhalla,[5] the differential RTEA cross section for a particular doubly excited state $|d\rangle$ deexciting to the ground state $|g\rangle$ by Auger electron emission is given by

$$\frac{d\sigma_{\mathrm{RTEA}}}{d\Omega}(d\rightarrow g,\theta)=\frac{J(Q_R)}{V_p\varepsilon_0}\Omega_{\mathrm{RE}}(d)\left[\frac{1}{4\pi}W(\theta)\right], \quad (1)$$

where

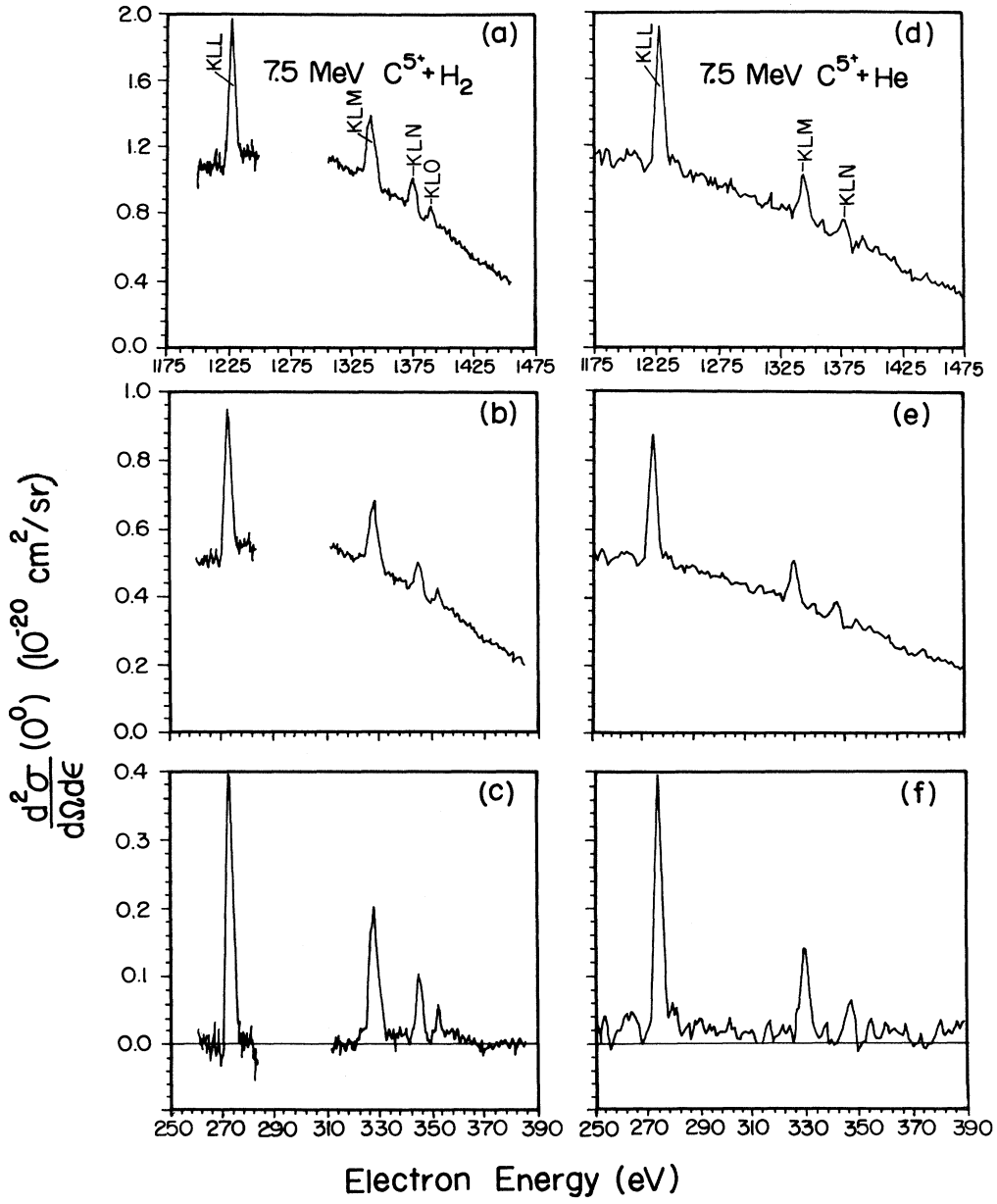

FIG. 1. Typical electron spectra for 7.5-MeV $C^{5+}+H_2$, He. (a) and (b) are the laboratory-frame electron yields. In (b) and (e), the laboratory-frame spectra have been transformed to the projectile frame. The normalized, transformed and binary electron background subtracted spectra are shown in (c) and (f).

$$\Omega_{\mathrm{RE}}(d)=\frac{2.475\times10^{-30}}{E_A}\frac{(2L_d+1)(2S_d+1)}{(2L_g+1)(2S_g+1)}\times\frac{A_a^2(d\rightarrow g)}{\sum_a A_a+\sum_r A_r}\mathrm{cm}^2\,\mathrm{eV}\ .$$

The orbital and spin angular momenta of the doubly excited state $|d\rangle$ and the ground state $|g\rangle$ are denoted by (L_d,S_d) and (L_g,S_g), respectively. E_A is the Auger electron energy in eV. A_a and A_r, the Auger rates and the radiative rates, are in s^{-1}. $W(\theta)$ depends on the resonance characteristics and the interference between the resonance and elastic scattering channels. We have performed explicit calculation of the relevant atomic parameters for all states with electron configurations $2lnl'$ for $n=2,3,4$. These calculations were performed using the Hartree-Fock atomic model by including the effects due to configuration interactions. The results for $\Omega_{\mathrm{RE}}(d)$ and

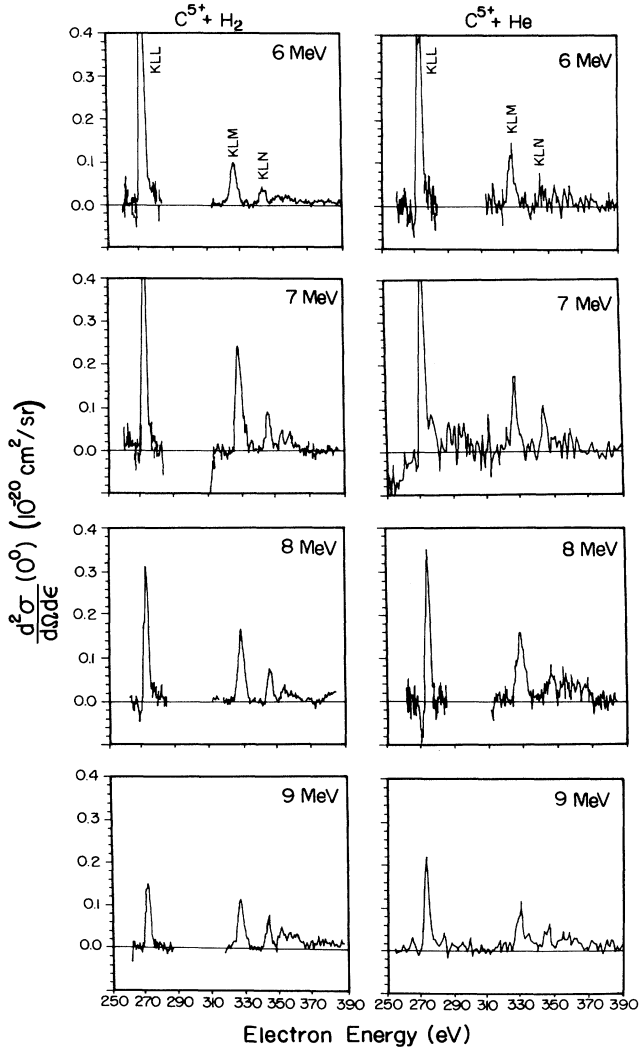

FIG. 2. High-resolution electron spectra for 6-, 7-, 8-, and 9-MeV $C^{5+}+H_2$, He.

TABLE I. Theoretical parameters for the doubly excited C^{4+} states ($2lnl'$), the Auger energy E_A (eV), Ω_{RE} (10^{-19} cm^2 eV), anistropy factor $W(\theta_{\mathrm{lab}}=0)$.

Doubly excited state	E_A	Ω_{RE}	$W(\theta_{\mathrm{lab}}=0)$
$2s^2\,{}^1S$	263.6	14.49	0.81
$2p^2\,{}^1D$	273.3	66.41	5.31
$2s2p\,{}^1P$	274.5	22.18	1.57
$2p^2\,{}^1S$	282.6	0.51	1.81
$2s3p\,{}^3P$	325.4	1.66	1.60
$2s3s\,{}^1S$	326.8	4.61	0.84
$2p3d\,{}^3F$	327.3	2.00	7.50
$2s3d\,{}^3D$	327.5	0.74	5.61
$2p3p\,{}^1D$	328.9	12.51	5.49
$2p3s\,{}^1P$	329.8	7.30	1.67
$2s3d\,{}^1D$	330.4	12.20	5.49
$2p3d\,{}^1F$	330.7	3.64	7.40
$2p3d\,{}^1P$	331.3	1.35	1.61
$2s4p\,{}^3P$	344.4	0.92	1.55
$2s4s\,{}^1S$	345.0	2.08	0.87
$2p4d\,{}^3F$	345.3	0.64	7.48
$2s4d\,{}^3D$	345.4	0.19	5.70
$2p4p\,{}^1D$	345.9	4.68	5.51
$2p4s\,{}^1P$	346.1	2.67	1.68
$2s4d\,{}^1D$	346.5	4.66	5.54
$2p4d\,{}^1F$	346.6	1.73	7.34
$2p4d\,{}^1P$	346.9	0.48	1.54

$W(\theta_{\mathrm{lab}}=0)$ are presented in Table I. The Compton profile of the target is denoted by $J(Q)$, the projectile velocity by V_p, and ϵ_0 is the atomic unit of energy. E_I is the ionization energy of the target electron and Q_R is defined by

$$Q_R=\frac{E_A+E_I}{\epsilon_0 V_p}-\tfrac{1}{2}V_p\ .$$

Since the different Auger lines could not be resolved within each group KLn, we define

$$\frac{d\sigma}{d\Omega}(KLn)=\sum_d\frac{d\sigma_{\mathrm{RTEA}}}{d\Omega}(d\rightarrow g,\theta=0)\qquad(2)$$

in order to compare with data. The summation is over the doubly excited states in each KLn group. It is also convenient to define RTEA resonance strengths as follows for each group:

$$\sum_R(KLn)=\int\frac{d\sigma}{d\Omega}(KLn,\theta=0)dE_p\qquad(3)$$

for the range of projectile energies.

IV. RESULTS AND DISCUSSIONS

Differential KLL, KLM, and KLN cross sections are displayed as a function of projectile energy for H_2 and He in Figs. 3 and 4, respectively. The relative uncertainty, indicated by the error bars in the figures, is approximately 15%. These were determined by adding in quadrature the statistical error to the uncertainty due to background subtraction and fitting.

The solid curves are the theoretical predictions for RTEA, generated by summing the contributions of all the possible lines in each of the *KLL*, *KLM*, and *KLN* manifolds and folding these into H_2 and He Compton profiles. The possible contributions of nonresonant transfer excitation[8,9] (NTE), which are not expected to be significant for the system studied here, have been ignored in the present theoretical results. The theory curves have been multiplied by an arbitrary factor in the range 0.65±0.05 to fit the data for all the cases.

The process of RTE, according to Eq. (1), simply reflects the Compton profile of the target electrons. The area under the RTEA resonance curve can be integrated over the range of projectile energy yielding RTEA resonance strengths, Σ_R as defined in Eq. (3). In Fig. 5, the

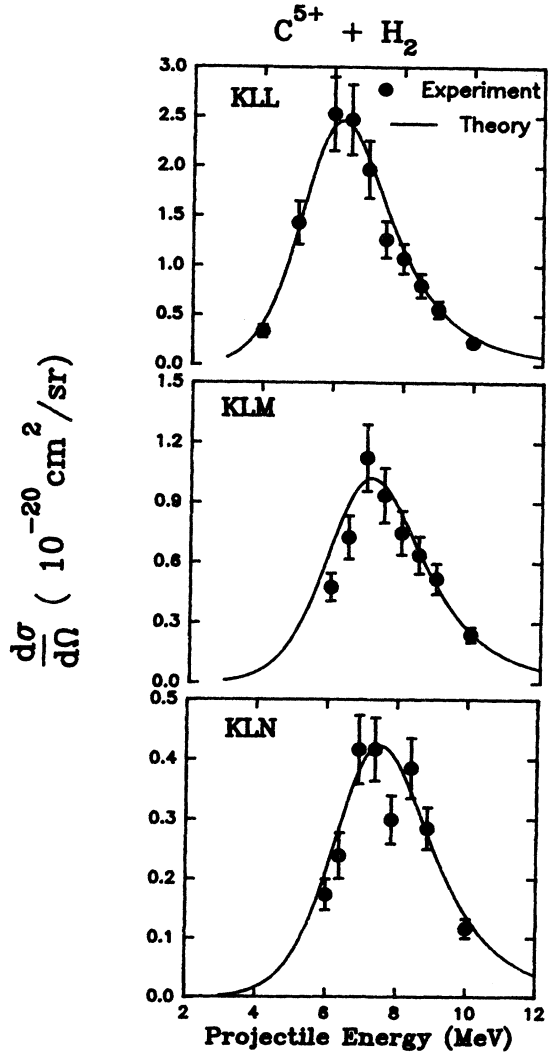

FIG. 3. Differential TE cross sections for $C^{5+}+H_2$. The solid curves are the RTEA theoretical predictions generated by summing all the different lines in each *KLn* manifold. The theory has been multiplied by an arbitrary constant in the range 0.65±0.05 to fit the data in all the cases.

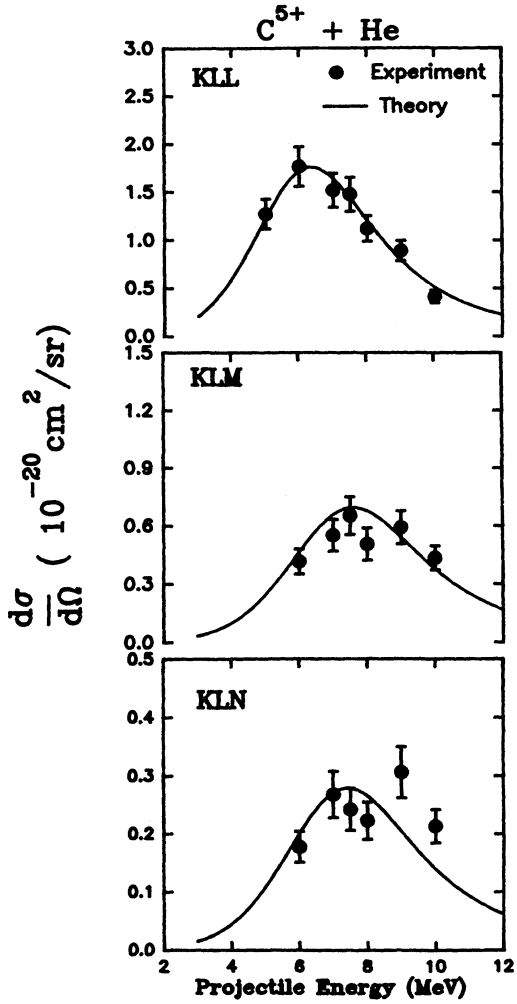

FIG. 4. Differential TE cross sections for $C^{5+}+He$. The solid curves are the RTEA theoretical predictions generated by summing all the different lines in each *KLn* manifold. The theory has been multiplied by an arbitrary constant in the range 0.65±0.05 to fit the data in all the cases.

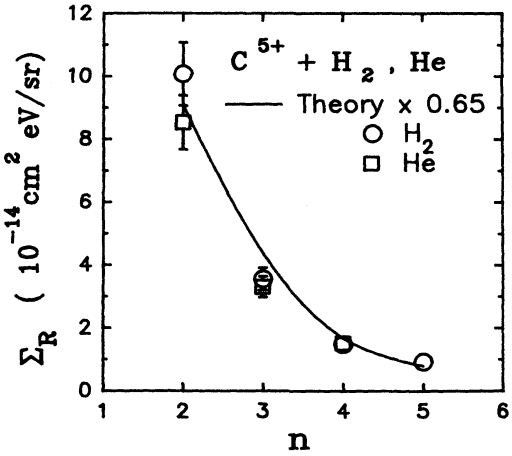

FIG. 5. The RTEA resonance strengths generated by integrating under the theory and experimental points in Figs. 3 and 4, over the range of projectile energies. The theory points have been uniformly multiplied by 0.65.

KLn RTEA resonance strengths estimated from Figs. 3 and 4 are plotted as a function of n, the principal quantum number. The experimental resonance strengths were generated by fitting smooth curves through the data points and integrating over the projectile energy range. The theoretical resonance strengths were obtained by integrating under the theory curves and have been uniformly multiplied by 0.65.

V. SUMMARY

We have studied the RTEA process for $C^{5+}+H_2$ and He collision systems. The resolution of the experiment was sufficient to determine the *KLL*, *KLM*, *KLN*, and *KLO* differential RTEA cross sections without resolving the individual Auger lines in each manifold. Theoretical calculations using the Hartree-Fock atomic model for the differential cross sections are also presented. Resonance strengths for RTEA are determined experimentally and compared with theory. Agreement is very good except for an absolute normalization factor. The experimental values for the differential cross section are found to be smaller than theoretical prediction by about 35%, consistent with previously observed *KLL* RTEA cross-section results.[3,4] This suggests the need for further experiments with different systems in order to resolve the discrepancy and to test the applicability of the currently used impulse approximation.

ACKNOWLEDGMENT

The authors would like to acknowledge the support of the Division of Chemical Sciences, Office of Basic Energy Sciences, Office of Energy Research, U.S. Department of Energy in this work.

[1]A. Itoh, T. J. M. Zouros, D. Schneider, U. Stettner, W. Zeitz, and N. Stolterfoht, J. Phys. B **18**, 4581 (1985); J. K. Swenson, Y. Yamazaki, P. D. Miller, H. F. Krause, P. F. Dittner, P. L. Pepmiller, S. Datz, and N. Stolterfoht, Phys. Rev. Lett. **57**, 3042 (1986).

[2]W. G. Graham, K. H. Berkner, E. M. Bernstein, M. W. Clark, B. Feiberg, M. A. McMahan, T. J. Morgan, W. Rathburn, A. S. Schalcter, and J. A. Tanis, Phys. Rev. Lett. **65**, 2773 (1990), and references therein.

[3]T. J. M. Zouros, C. P. Bhalla, D. H. Lee, and P. Richard, Phys. Rev. A **42**, 678 (1990).

[4]B. D. DePaola, R. Parameswaran, and W. J. Axmann, Phys. Rev. A **41**, 6533 (1990).

[5]C. P. Bhalla, Phys. Rev. Lett. **64**, 1103 (1990).

[6]M. Schulz, J. P. Giese, J. K. Swenson, S. Datz, P. F. Dittner, H. F. Krause, H. H. Schone, C. R. Vane, M. Benhenni, and S. M. Shafroth, Phys. Rev. Lett. **62**, 1738 (1989).

[7]R. Parameswaran, W. J. Axmann, T. J. M. Zouros, and B. D. DePaola, Nucl. Instrum. Methods B **40/41**, 158 (1989).

[8]D. Brandt, Phys. Rev. A **27**, 1314 (1983).

[9]J. M. Feagin, J. S. Briggs, and T. M. Reeves, J. Phys. B **17**, 1057 (1984); D. Brandt, Nucl. Instrum. Methods **214**, 93 (1983); Y. Hahn, Phys. Rev. A **40**, 2950 (1989).